Science of the Total Environment 811 (2022) 151619

Contents lists available at ScienceDirect

Science of the Total Environment

journal homepage: www.elsevier.com/locate/scitotenv

Net CO_2 and CH_4 emissions from restored mangrove wetland: New insights based on a case study in estuary of the Pearl River, China

Xiaosong Zhao [a,b], Chunlin Wang [b,c], Tingting Li [b,d,*], Chengyi Zhang [e,**], Xingwang Fan [a], Qing Zhang [d], Qiang Zhang [e], Xianyan Chen [e], Xukai Zou [e], Chong Shen [c], Yuqi Tang [f], Zhangcai Qin [b,g]

[a] Key Laboratory of Watershed Geographic Sciences, Nanjing Institute of Geography and Limnology, Chinese Academy of Sciences, Nanjing 210008, China
[b] Southern Marine Science and Engineering Guangdong Laboratory (Zhuhai), Zhuhai 519000, China
[c] Guangzhou Climate and Agrometeorology Center, Guangzhou 510080, China
[d] State Key Laboratory of Atmospheric Boundary Layer Physics and Atmospheric Chemistry, Institute of Atmospheric Physics, Chinese Academy of Sciences, Beijing 100029, China
[e] National Climate Center, China Meteorological Administration, Beijing 100081, China
[f] School of Atmospheric Sciences, Nanjing University, Nanjing 210023, China
[g] School of Atmospheric Sciences, Guangdong Province Key Laboratory for Climate Change and Natural Disaster Studies, Sun Yat-sen University, Zhuhai 519000, China

HIGHLIGHTS

- Mangrove wetland still as a carbon source after 12 years of restoration
- Carbon source was related to high ecosystem respiration over open waters.
- Carbon source intensity tended to decrease with the time of restoration.
- Global warming potential shows an intensified radiative warming effect.

GRAPHICAL ABSTRACT

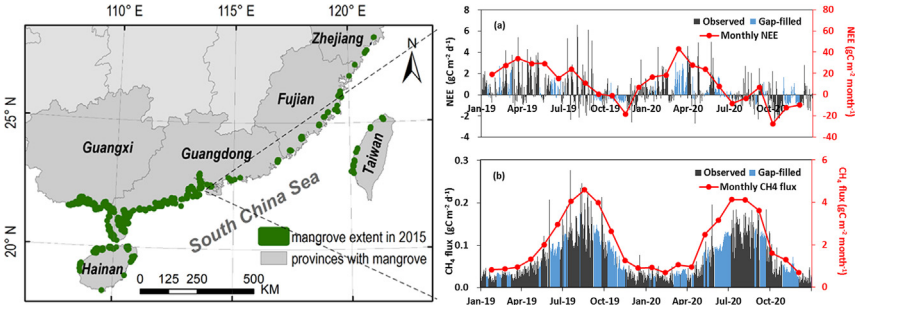

ARTICLE INFO

Article history:
Received 27 September 2021
Received in revised form 5 November 2021
Accepted 7 November 2021
Available online 12 November 2021

Editor: Pingqing Fu

Keywords:
Carbon exchange
Mangrove restoration
Southeast China
Eddy covariance
Random forest algorithm

ABSTRACT

Mangroves have the potential to affect climate via C sequestration and methane (CH_4) emissions. With half of the world's mangroves lost during the 20th century, mangrove restoration in mitigating greenhouse gases has been increasingly recognized. However, the carbon exchanges during restored processes still remain large uncertain. In this study, we analyzed the temporal variations of CO_2 and CH_4 fluxes and their environmental controls during 2019 and 2020 based on a closed-path eddy covariance (EC) system in a 12-year restored subtropical mangrove wetland, in estuary of the Pearl River, southeastern China. We also estimated the CO_2 and CH_4 fluxes and their climate effect from the beginning of restoration by Random Forest algorithm (RF). The EC observations showed that annually the 12-year restored mangrove acted as CO_2 and CH_4 sources, with net CO_2 ecosystem exchange (NEE) of 82–175 $gC \cdot m^{-2} \cdot a^{-1}$ and CH_4 fluxes of 24.7–26.3 $gC \cdot m^{-2} \cdot a^{-1}$. Low vegetation gross primary productivity (GPP) and high ecosystem respiration (Re) caused net CO_2 emissions in the mangroves. The estimation by RF indicated that the mangroves were always a CO_2 source after the beginning of restoration, but the annual NEE was linearly decreased from 233 to 131 $gC \cdot m^{-2} \cdot a^{-1}$ from 2008 to 2020. The annual CH_4 emissions continually increased from 19.0 to 25.8 $gC \cdot m^{-2} \cdot a^{-1}$ after restoration. As a result, the restored mangrove had a positive effect on climate warming, with increased GWP from 1276 to 1386 g CO_2-eq $\cdot m^{-2} \cdot a^{-1}$ from 2008 to 2020. This is mainly due to lower GPP and higher Re by young restored

* Correspondence to: T. Li, State Key Laboratory of Atmospheric Boundary Layer Physics and Atmospheric Chemistry, Institute of Atmospheric Physics, Chinese Academy of Sciences, Beijing 100029, China.
** Corresponding author.
E-mail addresses: litingting@mail.iap.ac.cn (T. Li), zhangchy@cma.cn (C. Zhang).

https://doi.org/10.1016/j.scitotenv.2021.151619

mangroves, large water area as well as low salinity induced strong CH_4 emissions. Our results indicate new sights that young restored mangrove with large area of water surface may act as carbon sources. However, the long-term climate and ecosystem benefits due to mangrove restoration should not be ignored in future.

1. Introduction

Coastal wetlands own the capability to capture and storage carbon, known as blue carbon, and thus have the potential of reducing global atmospheric carbon dioxide (CO_2) concentrations (Duarte et al., 2013; Macreadie et al., 2017). Mangroves have the highest carbon sequestration rate among all other natural ecosystems (Donato et al., 2011; Friess et al., 2019; Taillardat et al., 2018). Although mangroves occupy only 0.5% of the global coastal area, their disproportionate contribution to carbon sequestration has a significant effect on global carbon budget and climate change mitigation (Duarte et al., 2013; Nellemann et al., 2009).

The carbon budget of mangrove wetland ecosystem includes the greenhouse gas (GHG) net exchange of CO_2 and CH_4 between mangrove vegetation, soil and atmosphere (Jennerjahn et al., 2017). The CO_2 can be sequestrated by wetland plants through photosynthesis (Choi et al., 2001). Gaseous carbon release in wetlands mainly includes CH_4 emissions from microbial methanogenic processes (Singh et al., 2000), and CO_2 emissions from plant respiration, sediment heterotrophic respiration, and sediment chemical processes (Roehm, 2005). With the eddy covariance (EC) technique widely used in quantification of biosphere-atmosphere carbon exchange in various ecosystems (Baldocchi, 2014), a growing number of studies have examined ecosystem-scale CO_2 fluxes in mangroves using EC measurements (Barr et al., 2010; Chen et al., 2014; Cui et al., 2018; Leopold et al., 2016; Liu and Lai, 2019; Rodda et al., 2016). Current studies show that the annual net CO_2 uptake of coastal mangroves ranges from −249 to −891 g CO_2-C·m^{-2} (Alvarado-barrientos and López-adame, 2020; Chen et al., 2014; Liu and Lai, 2019; Rodda et al., 2016). Although mangroves are a weak CH_4 source, the strong greenhouse effect cannot be ignored. The annual CH_4 flux from mangroves ranges from 11.1–20.3 g CH_4-C·m^{-2} (Holm et al., 2016; Knox et al., 2019; Krauss et al., 2016), which may offset approximately 20–50% of the negative radiative forcing caused by CO_2 uptake over a 20-year timescale (Liu et al., 2020; Rosentreter et al., 2018b). Therefore, mangrove CO_2 uptake and CH_4 emission should be synchronously considered to comprehensively evaluate the impact of carbon exchange on climate change.

The past decades of coastal population increase and economic development have decreased the mangrove area by approximately 30–50% (Donato et al., 2011; Duke et al., 2007; Friess et al., 2019). Since the 1970s, mangrove forest conservation has attracted an increasingly international interest, in recognition of the essential value of climate mitigation through carbon storage, coastal protection and biodiversity conservation (Atwood et al., 2017; Hamilton and Friess, 2018; Hochard et al., 2019; Sievers et al., 2019). The Global Mangrove Alliance plans to restore 20% of the world's mangrove area by 2030 (Friess et al., 2019). This presents an unprecedented opportunity for mangroves restoration.

Global mangrove deforestation resulted in C release of 0.02–0.12 Pg·C·a^{-1} into the atmosphere, accounting for about 10% of global CO_2 emissions from deforestation (Donato et al., 2011). Mangrove recovery following disturbances usually absorbs C from atmosphere to partially compensate the C losses caused by disturbance (Sasmito et al., 2019). Some existing GHG reduction schemes (e.g., Reduced Emissions from Deforestation and Degradation and Global Commission on Adaptation) and Nationally Determined Contribution (NDC) have prioritized mangrove conservation and restoration in their climate mitigation effect (Gallo et al., 2017; Lovelock and Duarte, 2019). However, there is still a large knowledge gap in the carbon cycling process after mangrove restoration. On one hand, the processes vary significantly depending on location, climate, sediment type, coastal geomorphology, as well as methods of regeneration or reforestation (Adame et al., 2018; Phan et al., 2019; Sasmito et al., 2019; Schile et al., 2017). On the other hand, the plant biomass accumulation rates and soil carbon sequestration rates change in different stages of restoration, which also impacts carbon exchange in association with autotrophic respiration and heterotrophic respiration (Fu et al., 2017).

China has experienced significant dynamics in mangrove area, decreasing from ~40,000 ha in 1950s (Fan and Liang, 1995) to 13,000–20,000 ha (Jia et al., 2018) in 1990s. Saltworks, croplands, and aquaculture ponds are the main driver of mangrove loss (Temmerman et al., 2013; Wang et al., 2014). Since 1990s, the Chinese government has made great efforts in mangrove restoration with 4000 ha restored, mainly in the form of natural reserve and mangrove park (Jia et al., 2018). However, only about 57% of the restored mangroves survived (Chen et al., 2009). Wetland parks are generally under good management, free from tidal influence and environmentally stable, which largely improve the mangroves' survival rate. Previous studies usually focused on carbon exchanges in natural mangroves in China (Chen et al., 2010; He et al., 2019; Li et al., 2014; Zhu et al., 2021), whereas much less attention has been paid on carbon exchanges during mangrove restoration processes.

In this study, we used EC measurements and random forest algorithm to investigate carbon exchanges of a 12-year-old restored mangrove wetland in Guangzhou, Guangdong province, China. We hypothesized that mangrove carbon uptake could offset CH_4 emission, CO_2 release from plants, water and soil respiration, rendering the wetland as carbon neutral or weak carbon sink after 12-year restoration. The primary objectives are: (1) to characterize temporal variations in carbon exchange (including CO_2 and CH_4 fluxes) and reveal the biophysical drivers, and (2) to assess the age-related trend of net carbon budget after restoration. This study might provide key information regarding future restoration of mangrove wetlands, and provide an insight into local carbon balance.

2. Materials and methods

2.1. Study sites

The study site (22.60°N, 113.64°E, Fig. 1) is located within the Nansha coastal wetland park, Guangzhou, China. Belonging to a subtropical marine monsoon climate, the site has an annual mean temperature of 21.8 °C, and an annual mean precipitation of 1635.6 mm (Qiu et al., 2011). The dominant wind direction is northwest in winter and southeast in summer. Nansha wetland belongs to the estuarine wetland of the low sediment plain, which is transformed by artificial reclamation into a tidal flat raised by continuous siltation of sand and mud from rivers and oceans.

The park has a total area of about 6.54 km^2, including Zone I (about 2.4 km^2) restored from 1994, and Zone II (about 4.1 km^2) restored from 2008 (Fig. 1c). Our eddy covariance (EC) system is located within the Zone II (more details see Section 2.2). The mangrove community is dominated by the *Hibiscus tiliaceus* (70%) and the *Sonneratia apetala* (17%). The *H. tiliaceus* community has a canopy height of 3–4 m, and a canopy density of 0.7–0.8. The mangrove stands are planted in striped

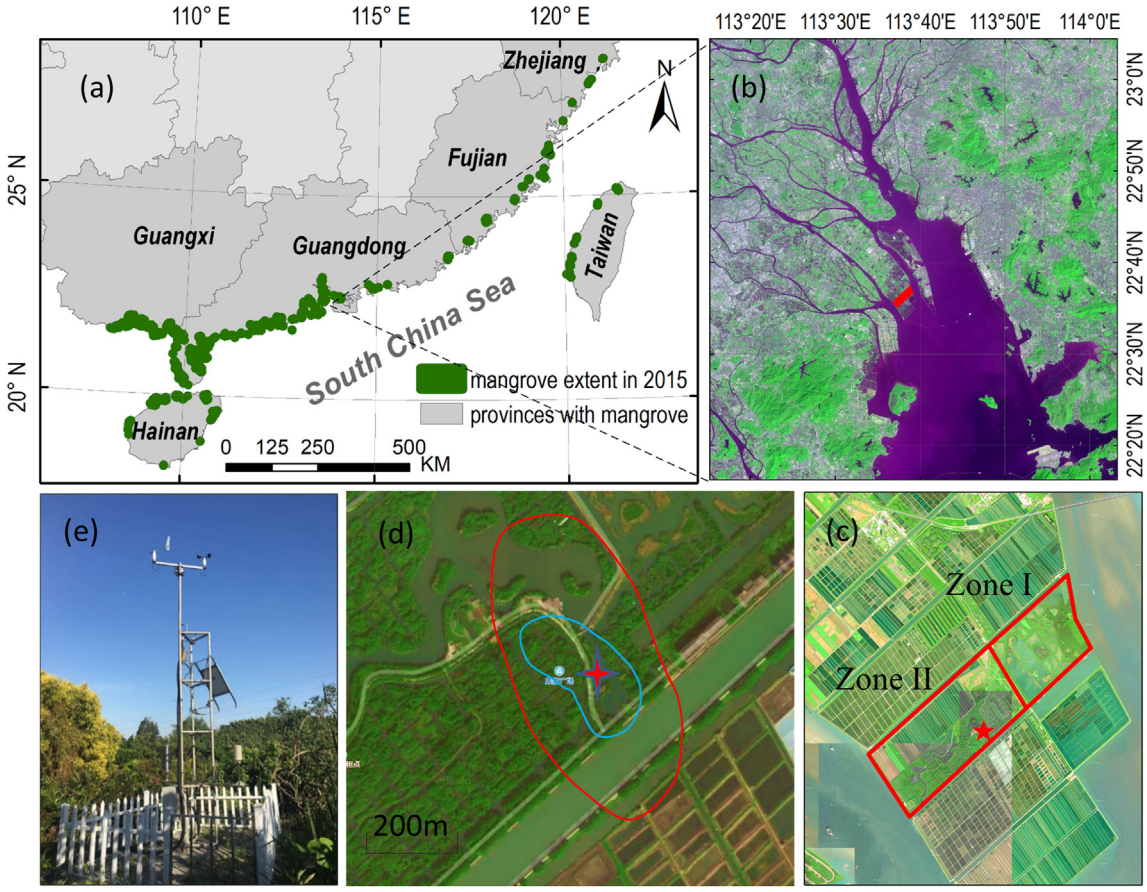

Fig. 1. Illustration of study site and EC system including (a) mangrove distribution in China (data from Jia et al., 2018), (b) the Pearl River mouth, (c) location of the Nansha wetland park including Zone I and Zone II, with red star showing the location of EC system, (d) land surface conditions of 90% flux source area (blue for 5-m tower, red for 10-m tower), and (e) photo of EC system.

shapes surrounded by open waters. The proportion of vegetation canopy is about 60%. Water level is regulated with minor fluctuations.

The wetland is located at the junction of saline and fresh water at the mouth of the Pearl River (Fig. 1b). The waters are saline from October to the next March, with a salinity level between 1‰ and 8‰. In dry season (January), the average PH, dissolved oxygen and total nitrogen are 8.2, 8.95 $mg \cdot l^{-1}$ and 0.73 $mg \cdot l^{-1}$, and in wet season (June), the indices values are 7.6, 5.19 $mg \cdot l^{-1}$ and 0.6 $mg \cdot l^{-1}$ (Song et al., 2016).

2.2. EC and meteorological observations

An EC system was installed on a 5-m tower in the center of the wetland park (Fig. 1). The system consisted of a close-path infrared gas analyzer (GGA, ABB-Los Gatos Research, USA) and a three-dimensional sonic anemometer (WindMaster Pro, Gill Instruments, USA). The H_2O, CO_2 and CH_4 flux measurements were recorded by a CR3000 datalogger at a 10 Hz frequency. The air temperature (Ta, °C), relative humidity (RH, %) (HMP155, Vaisala, Finland), wind speed (WS) and wind direction (WD) (03002, RM Young, Inc. USA) were also measured. Soil temperature (Ts, °C) (109, Campbell Scientific, Inc. USA) and soil moisture (SWC, $cm^{-3} \cdot cm^{-3}$) (CS616, Campbell Scientific, Inc. USA) were measured at 5 cm and 10 cm below soil surface. The soil salinity (Hydra Prob 2, Campbell Scientific, Inc. USA) was also measured at 5 cm below soil surface for a few months. All measurements were averaged within 30 min and recorded by a CR1000 datalogger. Water level and water temperature (CS456, Campbell Scientific, Inc. USA) were also measured at a 30-min frequency. The water level probe was installed below water surface inside a 1-m tube.

Data were collected in the full years of 2019 and 2020. Before June 2020, the EC system was mounted at a 5-m height. The fluxes footprint included mangrove stands and open waters (Fig. 1d), covering a radius of 100–200 m according to Kljun et al. (2015). As mangrove stands grew, the canopy approached the 5-m tower, narrowing down the flux source areas. To meet EC flux observation requirements and keep the representativeness of underlying surfaces, the tower was adjusted to 10-m in June 2020. Then, the system was raised to a 10-m height. The footprint included part of ponds (Fig. 1d), extending to a radius of 500–600 m.

Additional 30-min meteorological data were obtained from a nearby (within 1 km) standard meteorological station (Shijiuyong). Solar radiation data were collected from the Guangzhou national meteorological station (23°08′N, 113°19′E). These data were used for gap-filling. The 16-day Normalized Difference Vegetation Index (NDVI) data were extracted from the MOD13Q1/MYD13Q1 product (250 m).

2.3. Flux data processing and gap-filling

Post-processing of flux data followed the FLUXNET standard procedures based on the EddyPro software v6.1.0. First, screening and despiking was performed following Vickers and Mahrt (1997). The angle-of-attack correction recommended for Gill anemometers was applied (Nakai and Shimoyama, 2012). Then, double coordinate rotation was applied to the raw horizontal and vertical wind components (Wilczak et al., 2001). Time lags between the anemometric and gas analyzer's measurements were detected and compensated via the covariance maximization procedure (Fan et al., 1990). In addition, the spectral response corrections were conducted (Massman, 2000; Moncrieff et al., 2004). The WPL (Webb, Pearman, and Leuning) correction was performed to correct for air density fluctuations (Webb et al., 1980). The friction velocity (u*) threshold of 0.1 $m \cdot s^{-1}$ was determined by using

the moving point testing method (Reichstein et al., 2005). Finally, 33% of CO_2 flux data and 38% of CH_4 flux data were removed, respectively.

The CO_2 and CH_4 fluxes were gap-filled by using the eddy covariance gap-filling & flux-partitioning tool (http://www.bgc-jena.mpg.de/~MDIwork/eddyproc/index.php) (Reichstein et al., 2005; Wutzler et al., 2018). This tool fills flux data gaps by using look-up table and mean diurnal course methods (Wutzler et al., 2018), and partitions CO_2 fluxes (i.e., net ecosystem CO_2 exchange, NEE) into Gross Primary Productivity (GPP) and ecosystem respiration (Re). The nighttime partitioning method was used to partition NEE (Reichstein et al., 2005). The method develops a relationship between soil temperature and nighttime Re, and assumes that this relationship is also applicable to daytime Re.

The global warming potential (GWP) was introduced to evaluate the potential contribution of gaseous carbon balance to climate change. GWP is the time-integrated radiative forcing due to a pulse emission of a given gas relative to an equal mass of CO_2 (IPCC, 2014), which quantifies the potential contribution of non-CO_2 greenhouse gases on climate change in terms of "equivalent CO_2" (IPCC, 2014). In this study, we used the GWP value provided by the IPCC (2014) on a 100-year scale, which is 28 for CH_4 (i.e., 1 g CH_4 is equivalent to 28 g CO_2).

2.4. Random forest algorithm

Random Forest (RF) is a machine learning algorithm used to fit a large ensemble of regression trees to bootstrapped samples of a response variable, and the outputs of these trees are averaged to produce a simulated response. It can be used for regression, and to evaluate variables of importance (Breiman, 2001), widely applied in ecological studies, e.g., ecological model prediction (Archer and Kimes, 2008) and environmental factors importance analysis (Cutler et al., 2007). In this study, RF was used to model CO_2 and CH_4 fluxes based on environmental (hydrological, meteorological, biological) factors. The hydrological variables are water surface percentage (P_w) and land surface percentage (P_l). The meteorological variables are solar radiation (Ra), air temperature (Ta), daily temperature range (DT), relative humidity (RH), actual vapor pressure (e_a), vapor pressure deficit (VPD) and wind speed (WS). The only biological variable is NDVI. The model calibration/validation used all flux data that do not cover the pond area, 80% of which were randomly selected for calibration and the rest for validation. RF modelling was executed for 200 times and the validation metrics included Pearl's correlation coefficient (R), bias, standard deviation (SD) and root mean square error (RMSE).

The use of RF was two-folded in this study. First, RF was used to select variables of importance for CO_2 and CH_4 fluxes. Second, RF was used to reconstruct CO_2 and CH_4 fluxes in the wetland area from 2008 to 2020. For this purpose, a fixed P_w of 40% (P_l = 60%), and spatially averaged MODIS NDVI values were used.

3. Results

3.1. Climatic conditions and observed carbon fluxes

Featuring a typical subtropical monsoon climate, the site has a hot wet summer and a cool dry winter (Fig. 2). Daily air temperature (Ta) shows a clear seasonality ranging from 9.5 °C–32.1 °C, and daily soil temperature (Ts) shows less day-to-day variabilities than Ta. The mean Ta was 24.2 °C in 2019, slightly higher than 23.9 °C in 2020 (Fig. 2a). Daily VPD fluctuates from 0.02–1.65 kPa, and peaks in summer and autumn with lower precipitation and higher Ta (Fig. 2b). Daily solar radiation (Ra) showed a unimodal pattern in 2019, with maximum values in August. However, a M-shaped pattern was observed in 2020, with low values in July due to continuous precipitation (Fig. 2c). NDVI usually peaks in September to October and minimizes in March (Fig. 2d). The annual precipitation was 2085 mm in 2019 and 1356 mm in 2020. More than 85% precipitation was concentrated in April to September.

NEE shows large fluctuations, ranging between −2.9 and 6.6 $gC \cdot m^{-2} \cdot d^{-1}$, positive ($CO_2$ emission) in most time, and negative (CO_2 uptake) sporadically in every month (Fig. 3a). High CO_2 emission (2–6 $gC \cdot m^{-2} \cdot d^{-1}$) occurred before August. The source areas of daily NEE consist of 20%–40% open waters and 60%–80% mangroves before July 2020, and partly of 5%–10% ponds after July 2020 (Fig. 3c). Although GPP showed a strong carbon uptake (−0.5 to −7.1 $gC \cdot m^{-2} \cdot d^{-1}$) before August (Fig. S1), Re (2.8–7.0 $gC \cdot m^{-2} \cdot d^{-1}$) offset and surpassed it in most days, and finally carbon release was dominant before August 2019. Monthly NEE was positive before August 2019 and before June 2020 (Fig. 3a), with maximum values of 33.9 and 43.0 $gC \cdot m^{-2} \cdot month^{-1}$ in March of 2019 and 2020, respectively. Then, CO_2 uptake (−2.6 to −0.2 $gC \cdot m^{-2} \cdot d^{-1}$) dominated. Monthly NEE was negative in Sept.–Nov. 2019 and in Jul.–Dec. 2020 (Fig. 3a). The maximum CO_2 uptake occurred in November 2019 (−18.5 $gC \cdot m^{-2} \cdot month^{-1}$) and in October 2020 (−27.6 $gC \cdot m^{-2} \cdot month^{-1}$). The faster Re (relative to GPP) declining rate was responsible for negative NEE (Fig. S1). The total GPP was −1466 $gC \cdot m^{-2} \cdot a^{-1}$ and the total Re was 1641 $gC \cdot m^{-2} \cdot a^{-1}$ in 2019, leading to a net CO_2 source of 175 $gC \cdot m^{-2} \cdot a^{-1}$. In 2020, the total GPP was −1335 $gC \cdot m^{-2} \cdot a^{-1}$ and the total Re was 1417 $gC \cdot m^{-2} \cdot a^{-1}$, leading to a net CO_2 source of 82 $gC \cdot m^{-2} \cdot a^{-1}$. Lower GPP and higher Re is partly attributed to low vegetation cover (~60%) and high water surface cover (~40%) over the wetland park.

Daily CH_4 flux shows a clear seasonal pattern, higher fluxes in summer and lower fluxes in winter. Daily CH_4 flux ranges from 0.02–0.28 $gC \cdot m^{-2} \cdot d^{-1}$ (Fig. 3b). The source areas also come from ~40% open waters and ~ 60% mangroves, and partly of ~10% ponds after July 2020 (Fig. 3c). Monthly CH_4 flux maximized in August, 4.6 $gC \cdot m^{-2} \cdot month^{-1}$ in 2019 and 4.1 $gC \cdot m^{-2} \cdot month^{-1}$ in 2020. The minimum CH_4 flux occurred in January 2019 (0.8 $gC \cdot m^{-2} \cdot month^{-1}$), and in December 2020 (0.6 $gC \cdot m^{-2} \cdot month^{-1}$). Overall, the mangrove wetland acted as a CH_4 source of 26.3 and 24.7 $gC \cdot m^{-2} \cdot a^{-1}$, respectively in 2019 and 2020.

3.2. Environmental drivers of mangrove CO_2 and CH_4 fluxes

According to RF analysis, Ra is the most important variable for daily NEE, followed by RH, VPD and NDVI (Fig. 4). Daily GPP is mainly controlled by Ra, Ta and NDVI (Fig. S2), which are essential variables to vegetation photosynthesis. Both controlled by Ra, NEE and GPP share similar temporal variation patterns over the wetland park. Land surface percentage controls daily Re, indicating that vegetation exposure promotes ecosystem respiration. Daily Re is also related to Ta, e_a and NDVI, similar to Liu and Lai (2019) who report that soil respiration increases exponentially with soil temperature, air temperature and NDVI. Both GPP and Re are positively correlated with Ta, and their difference (NEE) shows a low correlation with Ta. The important variables are Ta, e_a and NDVI for daily CH_4 flux (Fig. 4b).

3.3. Carbon budget and GWP of restored mangrove

The RF performs well for modelling CO_2 flux (Fig. 5a). The modelling results are almost unbiased with a R value of 0.78, and SD and RMSE values less than 0.6 $gC \cdot m^{-2} \cdot d^{-1}$ (validation samples in Fig. 5b). The RF performs even better for modelling CH_4 fluxes (Fig. 5c). The unbiased modelling results have a R value of 0.9, and SD and RMSE values well within 0.05 $gC \cdot m^{-2} \cdot d^{-1}$ (validation samples in Fig. 5d).

Based on the RF simulation, the mangrove wetland park exhibits as CO_2 and CH_4 sources since restoration (Fig. 6a, b). The annual NEE shows a fluctuating downward trend from 233 to 131 $gC \cdot m^{-2} \cdot a^{-1}$ at a rate of −1.82 $gC \cdot m^{-2} \cdot a^{-1}$ (Fig. 6a), indicating a decreasing source of CO_2 after restoration. Although annual GPP and Re show a significant increasing trend (Fig. S3), the increasing rate of GPP (12.5 $gC \cdot m^{-2} \cdot a^{-1}$) is larger than that of Re (10.1 $gC \cdot m^{-2} \cdot a^{-1}$), leading to a net NEE decline

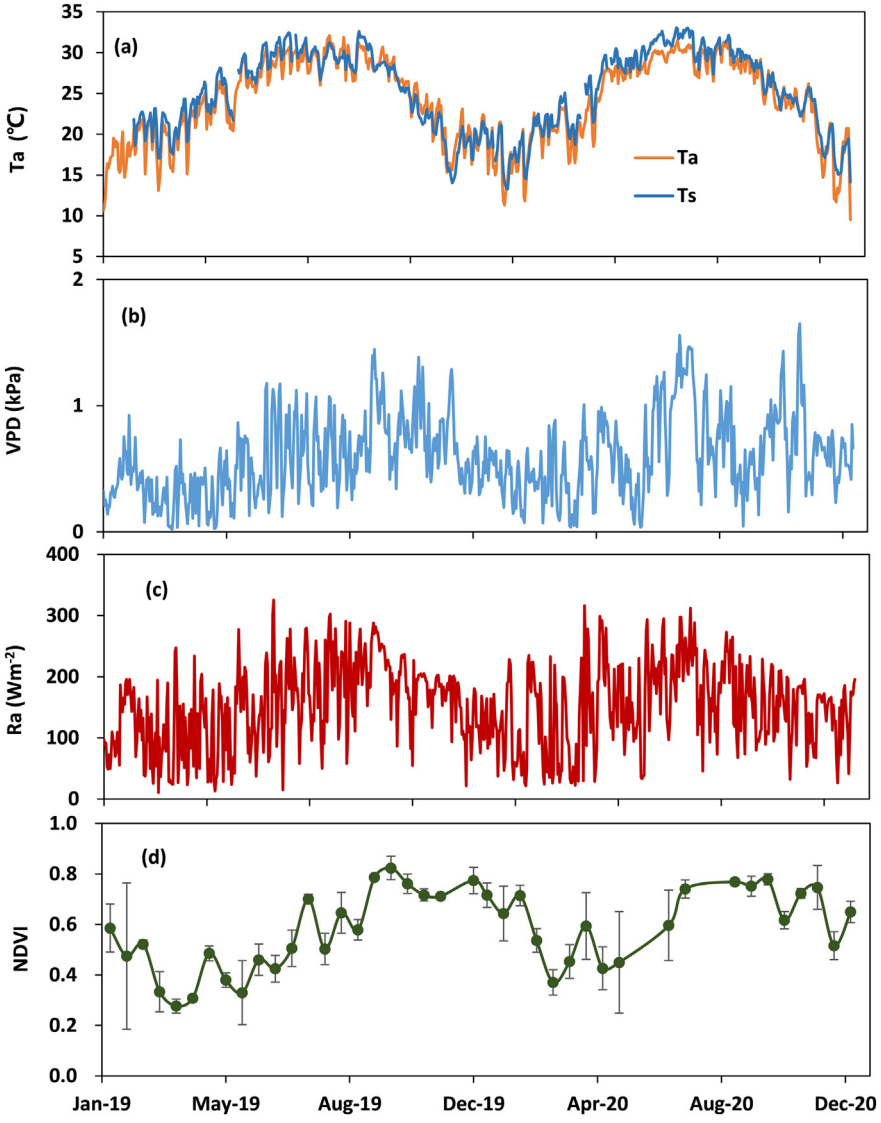

Fig. 2. Temporal variations in (a) daily air and soil temperatures (Ta, Ts), (b) daily vapor pressure deficit (VPD), (c) daily solar radiation (Ra), and (d) 16-day NDVI. Bars in (d) represent the standard deviation of all pixel values.

since 2008. The CH_4 flux shows a significant increasing trend from 19.0–25.8 $gCm^{-2}a^{-1}$ at a rate of 0.59 $gC{\cdot}m^{-2}{\cdot}a^{-1}$ (Fig. 6b).

The annual GWP induced by both CO_2 and CH_4 exchanges over the restored mangrove park increased from 1276 g CO_2-eq$\cdot m^{-2}\cdot a^{-1}$ in 2008 to 1386 g CO_2-eq$\cdot m^{-2}\cdot a^{-1}$ in 2020, at an increasing rate of 15.3 g CO_2-eq$\cdot m^{-2}\cdot a^{-1}$ (Fig. 6c). The mangrove park acted as both of CO_2 and CH_4 source, leading to intensive radiative warming effect. Despite the decrease in GWP caused by CO_2 emissions, the GWP of wetland parks still showed an increasing trend due to the 28-fold warming effect of CH_4on a 100-year time horizon.

The dominating variables of carbon fluxes differ between daily and annual scales. At annual scale, NEE is negatively related to Ra ($R^2 = 0.25$) and Ta ($R^2 = 0.22$). The environmental variables including Ra, Ta, and e_a showed an increasing trend from 2008 to 2020, especially for NDVI which increased sharply from 0.2 in 2008 to 0.6 in 2020 (Fig. S4). Annual GPP were promoted by annual Ta ($R^2 = 0.65$, $P < 0.01$), NDVI ($R^2 = 0.59$, $P < 0.01$) and e_a ($R^2 = 0.54$, $P < 0.01$) rising since 2008, and the increasing in annual Re was mainly caused by the increasing in NDVI ($R^2 = 0.48$, $P < 0.01$) and Ta ($R^2 = 0.37$). The annual CH_4 emission directly improved by NDVI ($R^2 = 0.83$, $P < 0.01$) then Ta ($R^2 = 0.6$, $P < 0.01$) increasing.

4. Discussion

4.1. CO_2 flux in mangrove

The role of coastal mangrove wetlands in sequestering atmospheric CO_2 and mitigating climate change has received increasing attention in recent years (Taillardat et al., 2018). Previous EC observations reported significant CO_2 sink in intact mangroves, with NEE ranges from −249 to −890 $gC{\cdot}m^{-2}{\cdot}a^{-1}$ for 3–6 m canopy height, and from −1105 to −1170 $gC{\cdot}m^{-2}{\cdot}a^{-1}$ for 12–20 m canopy height (Table 1). However, our EC observations show an opposite result in a 12-year restored mangrove wetland (Fig. 3a), with NEE ranges from 82 to 175 $gC{\cdot}m^{-2}{\cdot}a^{-1}$.

One reason for net CO_2 emission is the young mangrove stand age. Plant growth usually follows a slowly growing stage, a rapid growing stage and another slowly growing stage (Fu et al., 2017). The mangrove restoration efforts need 40 years to achieve biomass recovery (Sasmito et al., 2019). At the first stage, ecosystems have low photosynthetic capability and thus low GPP. The recovery rate of GPP might be lower than the increasing rate of Re. High Re to GPP ratio results in a net CO_2 source in the first 10 years (Goulden et al., 2011). This is consistent with our study. The current Re to GPP ratio

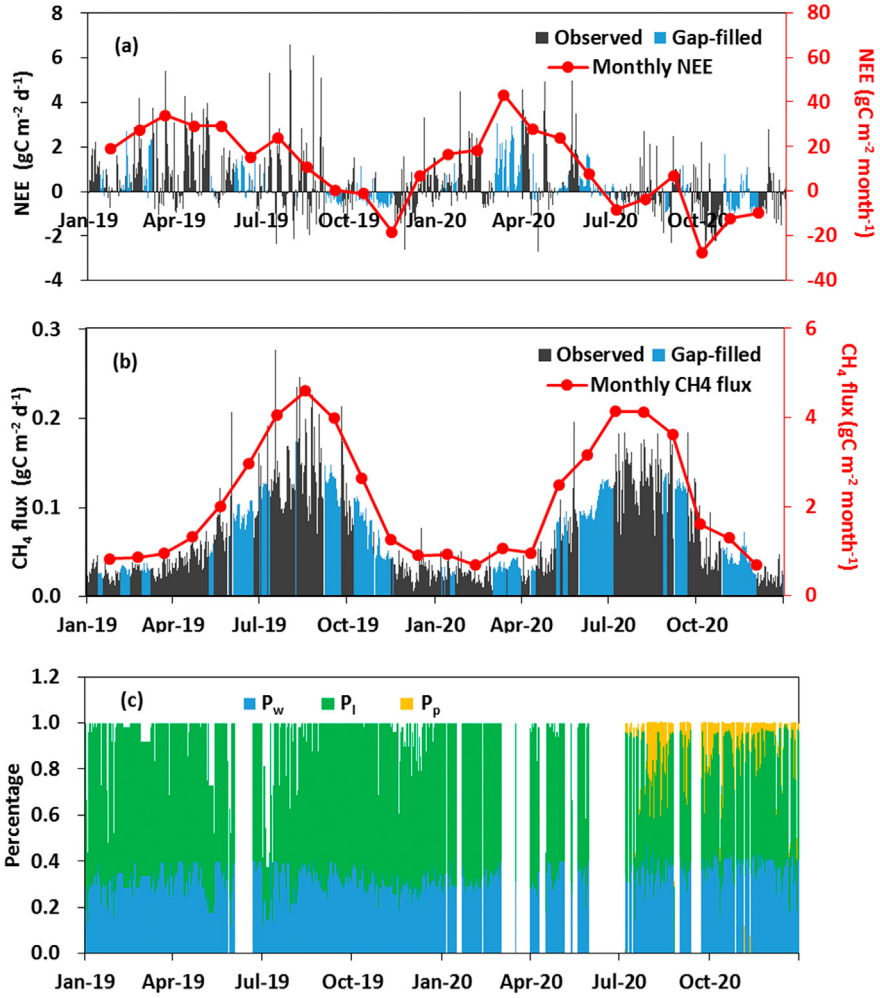

Fig. 3. Seasonal variations in daily and monthly (a) NEE and (b) CH_4 flux, and the daily water (P_w), land (P_l) and pond (P_p) components within EC source area.

(approximately 1.1) is significantly higher than the global average of 0.68 over intact mangroves with similar canopy height (Table 1). Our observations also show that the annual GPP ranges between −1335 and − 1466 $gC \cdot m^{-2} \cdot a^{-1}$, which fall in the lower end of similar mangroves (1271–2827 $gC \cdot m^{-2} \cdot a^{-1}$).

Another reason for net CO_2 emission is the distribution of open waters among mangrove stands. Small ponds and lakes (< 0.01 km2 in area) act as significant CO_2 sources, with a global mean NEE of 92 $gC \cdot m^{-2} \cdot a^{-1}$ (Deemer et al., 2016; Holgerson and Raymond, 2016). The ~40% surface water fraction in the wetland area (Fig. 3c) might contribute largely to CO_2 emission.

4.2. CH_4 flux in mangrove

Mangroves are generally considered as CH_4 sources (Rosentreter et al., 2018b), which is confirmed in this study over a 12-year restored

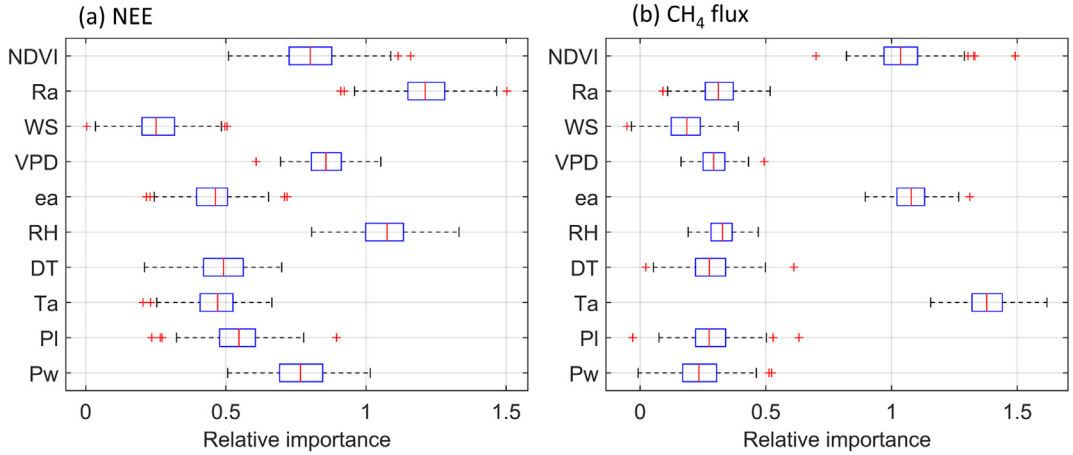

Fig. 4. Relative importance of explanatory variables for daily (a) NEE and (b) CH_4 flux. Results are presented as 200-time averages.

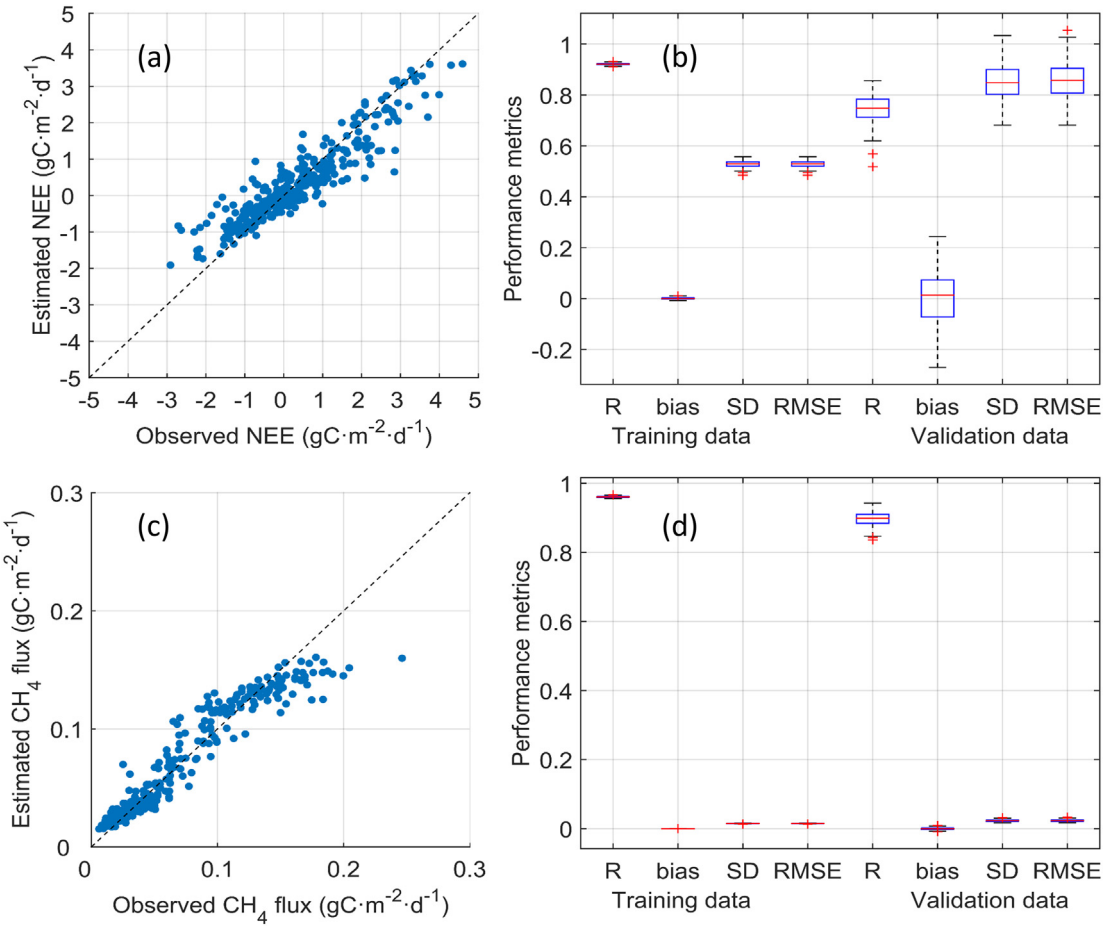

Fig. 5. RF performance for modelling CO_2 and CH_4 fluxes. The top row shows CO_2 modelling results and the bottom row shows CH_4 modelling results. The left column shows scatterplots for validation samples and the right column shows statistics.

mangrove. CH_4 fluxes vary substantially depending on environmental conditions (Rosentreter et al., 2018b). The global mangrove CH_4 fluxes range between −107.6 and 319.2 $gC \cdot m^{-2} \cdot a^{-1}$, with a median of 1.2 $gC \cdot m^{-2} \cdot a^{-1}$ (Al-Haj and Fulweiler, 2020). CH_4 emission in this study (24.7–26.3 $gC \cdot m^{-2} \cdot a^{-1}$) falls within the global range, yet is significantly larger than the median. All based on EC observations, the emission exceeds that of intact mangroves in the adjacent Fujian province (3.1 $gC \cdot m^{-2} \cdot a^{-1}$) and Hongkong (11.7 $gC \cdot m^{-2} \cdot a^{-1}$)(Liu et al., 2020; Zhu et al., 2021). Our result is comparable to the chamber method based observations in a nearby perennially flooding mangrove site (Kang et al., 2008). However, our result is significantly higher than those reported in other studies(Chen et al., 2010; Xu et al., 2020; Ye et al., 2000).

CH_4 production and oxidation from mangroves are controlled by physical and microbial processes, such as temperature and salinity gradients, water depth and water mixing, submarine groundwater discharge, organic matter respiration rates and the availability of terminal electron acceptors (Rosentreter et al., 2018a). Coastal wetland CH_4 emissions are also related to vegetation biomass and composition (Chen et al., 2010). CH_4 fluxes are controlled by Ta, e_a and NDVI at daily scale (Fig. 4b), while are significantly correlated with NDVI at annual scales, due to rapid NDVI increase (Fig. S4). Soil salinity inhibits CH_4 production in coastal wetlands, because electron acceptors such as NO^{3-} and SO_4^{2-} in coastal wetlands compete with the methanogens for electrons (Li et al., 2016; Poffenbarger et al., 2011). The soil salinity was always less than 1.0 ppb in our site, lower than the mangrove site in Fujian (5–20 ppb) (Zhu et al., 2021) and in Hongkong (5.3–13.9 ppb) (Liu et al., 2020). Lower salinity facilitates CH_4 emission in this study. In addition, non-flooding conditions decrease CH_4 emission, by developing aerobic environments and increasing soil redox potential (Ding et al., 2002; Li et al., 2010). Compared to the intermittently flooded mangrove sites in Fujian and Hongkong, our perennially flooded site benefits CH_4 emission.

4.3. Carbon budget in terms of GWP

Intact mangroves are believed to have significant climate benefits with negative GWP as high as −2500 g CO_2-eq $\cdot m^{-2} \cdot a^{-1}$ due to high net CO_2 uptake. Although CH_4 emission offsets 10–20% of the negative radiative forcing over 100-year time horizon, they still have strong climate cooling effect (Liu et al., 2020; Zhu et al., 2021). However, our study evidences that young restored mangroves may act as carbon a source, which contradicts our carbon neutral hypothesis. The reversal is caused by increased CH_4 emissions due to large-area low-saline open waters, lower GPP and higher respiration of young restored mangroves.

The construction of wetland restoration is expected to compensate for the carbon loss caused by LUCC in globally. However, the duration of ecosystem conversion to carbon sink is varied in different wetland types. A temperate riparian wetland after over 10-year restoration is still carbon source (Kandel et al., 2019). The 35-year-old restored mangroves appear to store similar levels of carbon to intact mangroves in the Mekong Delta (Ngoc et al., 2016). Mangrove restoration over 20 years acts as a strong CO_2 sink, with a mean NEE of −851 $gC \cdot m^{-2} \cdot a^{-1}$ (Table 1), attributable to large biomass of species (*Sonneratia apetala*)(Cui et al., 2018) and high planting densities

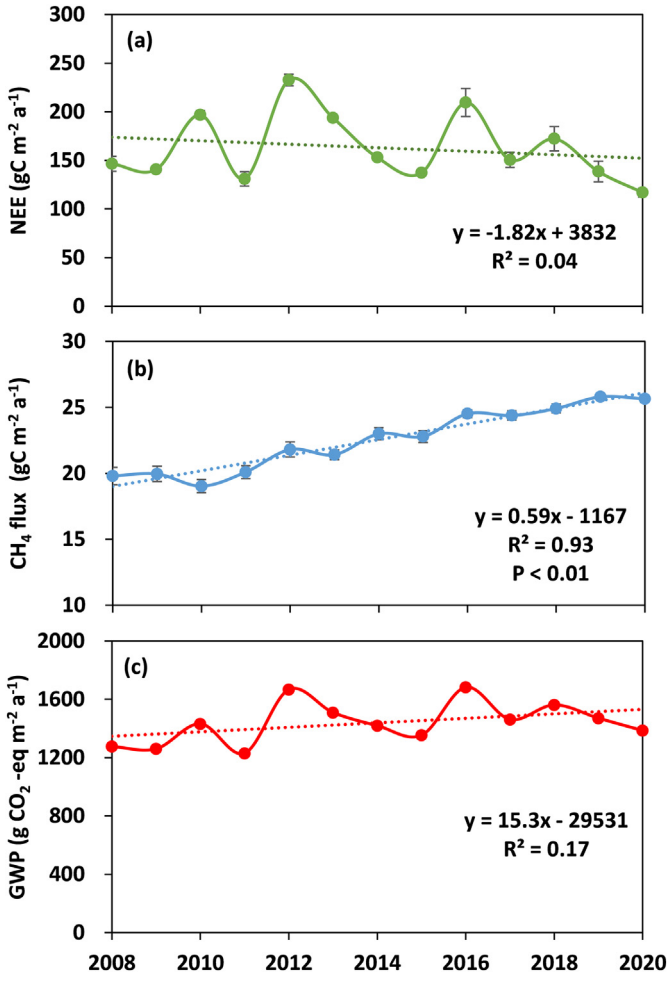

Fig. 6. Simulated annual (a) NEE, (b) CH_4 fluxes and (c) GWP over the mangrove wetland park since 2008.

(Liu et al., 2020). We find a decreasing trend of NEE from 2008 to 2020 (Fig. 6a), which is projected to offset the warming effect after a long-term restoration.

4.4. Uncertainties and future needs

Known limitations should be addressed to reduce uncertainties for further studies. First, several potential variables, e.g., tide level and salinity, are not considered due to lacking data. These variables are critical to carbon exchanges over mangroves (Li et al., 2016; Poffenbarger et al., 2011; Zhu et al., 2021). Second, the RF modelling will bring uncertainties, although this study used 10 parameters related with meteorology, hydrology and biology as inputs of RF method, it will still bring uncertainties when the prediction beyond the data range of the training set. For example, the RF in this study was based on the research area with the proportion of surface water around 20% - 40% (Fig. 3c) and daily NDVI above 0.2 (Fig. 2d). This method may bring uncertainties to estimate the mangroves with different water proportion or younger restored mangroves with NDVI less than 0.2. Long-term observations of other GHGs and additional environmental variables are necessary. Based on intensive observations, process-based models that describe biogeochemical processes of GHGs production, oxidation and transportation from mangroves may decrease uncertainties in long-term and large-scale prediction.

Wetland park plays an important role in habitat protection, environmental management, landscaping, ecotourism and recreation, which have been extensively evaluated. However, relatively less attention was paid to carbon budget. Our study showed that at the early stage of wetland park, carbon absorption of wetland vegetation usually cannot neutralize ecosystem respiration and CH_4 emissions, so the net carbon emission and their climate effects cannot be ignored. We suggest that future wetland park planning or mangrove restoration projects should place more considerations on biogeochemical factors. Vegetation species with stronger carbon sink capacity, planted at a large vegetation density, are recommended to maximize climate and ecosystem benefits.

Besides biogeochemical considerations, biophysical processes within wetland can also impact climate. Wetlands can significantly reduce surface albedo and surface temperature while increase evapotranspiration (Gao et al., 2014; Shen et al., 2020), which can offset the warming effects caused by greenhouse gas emissions. Future studies shall comprehensively consider both biogeochemical and biophysical processes at regional scales, to investigate the impact of wetland gain and loss on climate.

5. Conclusions

The closed-path eddy covariance system was used to continuously observe the CO_2 and CH_4 exchange from a 12-year restored estuary mangrove wetland in southeastern China during 2019 to 2020. The RF was used to reconstruct daily CO_2 and CH_4 fluxes in 2008–2020. The observations showed that the mangrove acted as both annual CO_2 and CH_4 sources. Lower GPP and higher respiration resulted in the CO_2 source. Large area of water surface and low salinity enhanced both CO_2 and CH_4 emissions. The simulated annual NEE showed a decrease trend, while the simulated annual CH_4 emissions showed an increase trend, which resulted in an increase GWP during the restored processes. The large water surface fraction in the wetland park impedes the accumulation of GPP, and promotes ecosystem respiration and CH_4 emission, which affect the advent of tipping point when the wetland park changes from carbon source to carbon sink. We further suggest that long-term continuous observations and process-based biogeochemical models are necessary to reduce uncertainties in estimating carbon

Table 1
Annual NEE, GPP and Re of mangrove ecosystem across the world.

Site	Location	P (mm)	Stand age	Canopy Height (m)	NEE ($gC \cdot m^{-2} \cdot a^{-1}$)	GPP ($gC \cdot m^{-2} \cdot a^{-1}$)	Re ($gC \cdot m^{-2} \cdot a^{-1}$)	Ref
Hongkang, China[a]	22.49°N, 114.3°E	1700	20–25	6.5	−758 to −890	−2741 to −2827	1983–1937	Liu and Lai (2019)
Yunxiao, China[b]	23.92°N, 117.41°E	1285	–	3–4	−540 to −857	−1762 to −1919	1238–1337	Chen et al. (2014)
Gaoqiao, China[b]	21.56°N, 109.75°E	1170	100	3	−692 to −738	−1698 to −1890	1027–1214	Chen et al. (2014)
Sundarban, India[b]	20.82°N, 88.61°E	1650	18–45	5	−249	−1271	1022	Ghosh et al. (2018); Rodda et al. (2016)
Quintana, Mexico[b]	20.84°N, 86.90°E	1222	–	5	−709	−2473	1764	Alvarado-barrientos and López-adame (2020)
Gulf, Mexico[b]	25.36°N, 81.07°W	1500	–	15–20	−1170	–	–	Barr et al. (2010)
Leizhou, China[a]	20.91°N, 110.09°E	1619	20	12	−1105	−2009	904	Cui et al. (2018)
Yunxiao, China[b]	23.92°N, 117.41°E	1715	–	3–6	−1076	−2197	1121	Zhu et al. (2021)
Nansha, China[a]	22.60°N, 113.64°E	1635	12	4–5	82–175	−1335 to −1466	1417–1641	This study

[a] Restored mangroves.
[b] Intact mangrove.

budget as well as its climate effect. Careful considerations about the landscape patterns and environmental factors should be paid attention during the mangrove restoration project in order to produce the best climate and ecosystem benefits.

CRediT authorship contribution statement

Xiaosong Zhao: Formal analysis, Writing – original draft, Visualization. **Chunlin Wang:** Investigation, Resources. **Tingting Li:** Conceptualization, Supervision, Resources. **Chengyi Zhang:** Conceptualization, Supervision, Resources. **Xingwang Fan:** Methodology, Data curation. **Qing Zhang:** Writing – review & editing. **Qiang Zhang:** Resources. **Xianyan Chen:** Investigation. **Xukai Zou:** Investigation. **Chong Shen:** Resources. **Yuqi Tang:** Resources. **Zhangcai Qin:** Writing – review & editing.

Declaration of competing interest

The authors declare that they have no known competing financial interests or personal relationships that could have appeared to influence the work reported in this paper.

Acknowledgment

This work was jointly supported by Guangzhou Basic Research Project (202002020076, 202002020065), the Open Research Fund of Ecological Meteorology Innovation for CMA Northeast Region (stqx201703), Guangdong Science and Technology Planning Project (2019B121201002), Guangdong Province Agricultural Science and Technology Innovation and Promotion Project (2021KJ102), the Comprehensive Monitoring of the Three Gorges Project (SK2021015), the National Natural Science Foundation of China (41975113, 41971046, 41775159, 42075020) and the Innovation Group Project of the Southern Marine Science and Engineering Guangdong Laboratory (Zhuhai) (311021001).

Appendix A. Supplementary data

Supplementary data to this article can be found online at https://doi.org/10.1016/j.scitotenv.2021.151619.

References

Adame, M.F., Zakaria, R.M., Fry, B., Chong, V.C., Then, Y.H.A., Brown, C.J., Lee, S.Y., 2018. Loss and recovery of carbon and nitrogen after mangrove clearing. Ocean Coast. Manag. 161. https://doi.org/10.1016/j.ocecoaman.2018.04.019.

Al-Haj, A.N., Fulweiler, R.W., 2020. A synthesis of methane emissions from shallow vegetated coastal ecosystems. Glob. Chang. Biol. https://doi.org/10.1111/gcb.15046.

Alvarado-barrientos, M.S., López-adame, H., 2020. Ecosystem-atmosphere exchange of CO2, Water, and energy in a basin mangrove of the Northeastern Coast of the Yucatan Peninsula. J. Geophys. Res. Biogeosci. 1–22. https://doi.org/10.1029/2020JG005811.

Archer, K.J., Kimes, R.V., 2008. Empirical characterization of random forest variable importance measures. Comput. Stat. Data Anal. 52. https://doi.org/10.1016/j.csda.2007.08.015.

Atwood, T.B., Connolly, R.M., Almahasheer, H., Carnell, P.E., Duarte, C.M., Lewis, C.J.E., Irigoien, X., Kelleway, J.J., Lavery, P.S., Macreadie, P.I., Serrano, O., Sanders, C.J., Santos, I., Steven, A.D.L., Lovelock, C.E., 2017. Global patterns in mangrove soil carbon stocks and losses. Nat. Clim. Chang. 7. https://doi.org/10.1038/nclimate3326.

Baldocchi, D., 2014. Measuring fluxes of trace gases and energy between ecosystems and the atmosphere - the state and future of the eddy covariance method. Glob. Chang. Biol. 20. https://doi.org/10.1111/gcb.12649.

Barr, J.G., Engel, V., Fuentes, J.D., Zieman, J.C., Halloran, T.L.O., Smith III, T.J., Anderson, G.H., 2010. Controls on mangrove forest - atmosphere carbon dioxide exchanges in western Everglades National Park. J. Geophys. Res. 115, 1–14. https://doi.org/10.1029/2009JG001186.

Breiman, L., 2001. Random forests. Mach. Learn. 45. https://doi.org/10.1023/A:1010933404324.

Chen, G.C., Tam, N.F.Y., Ye, Y., 2010. Summer fluxes of atmospheric greenhouse gases N2O, CH4 and CO2 from mangrove soil in South China. Sci. Total Environ. 408, 2761–2767. https://doi.org/10.1016/j.scitotenv.2010.03.007.

Chen, H., Lu, W., Yan, G., Yang, S., Lin, G., 2014. Typhoons exert significant but differential impacts on net ecosystem carbon exchange of subtropical mangrove forests in China. Biogeosciences 11, 5323–5333. https://doi.org/10.5194/bg-11-5323-2014.

Chen, L., Wang, W., Zhang, Y., Lin, G., 2009. Recent progresses in mangrove conservation, restoration and research in China. J. Plant Ecol. 2. https://doi.org/10.1093/jpe/rtp009.

Choi, Y., Wang, Y., Hsieh, Y.P., Robinson, L., 2001. Vegetation succession and carbon sequestration in a coastal wetland in Northwest Florida: evidence from carbon isotopes. Glob. Biogeochem. Cycles 15. https://doi.org/10.1029/2000GB001308.

Cui, X., Liang, J., Lu, W., Chen, H., Liu, F., Lin, Guangxuan, Xu, F., Luo, Y., Lin, Guanghui, 2018. Stronger ecosystem carbon sequestration potential of mangrove wetlands with respect to terrestrial forests in subtropical China. Agric. For. Meteorol. 249, 71–80. https://doi.org/10.1016/j.agrformet.2017.11.019.

Cutler, D.R., Edwards, T.C., Beard, K.H., Cutler, A., Hess, K.T., Gibson, J., Lawler, J.J., 2007. Random forests for classification in ecology. Ecology 88. https://doi.org/10.1890/07-0539.1.

Deemer, B.R., Harrison, J.A., Li, S., Beaulieu, J.J., Delsontro, T., Barros, N., Bezerra-Neto, J.F., Powers, S.M., Dos Santos, M.A., Vonk, J.A., 2016. Greenhouse gas emissions from reservoir water surfaces: a new global synthesis. Bioscience https://doi.org/10.1093/biosci/biw117.

Ding, W., Cai, Z., Tsuruta, H., Li, X., 2002. Effect of standing water depth on methane emissions from freshwater marshes in Northeast China. Atmos. Environ. 36. https://doi.org/10.1016/S1352-2310(02)00647-7.

Donato, D.C., Kauffman, J.B., Murdiyarso, D., Kurnianto, S., Stidham, M., Kanninen, M., 2011. Mangroves among the most carbon-rich forests in the tropics. Nat. Geosci. 4, 293–297.

Duarte, C.M., Losada, I.J., Hendriks, I.E., Mazarrasa, I., Marbà, N., 2013. The role of coastal plant communities for climate change mitigation and adaptation. Nat. Clim. Chang. 3, 961–968.

Duke, N.C., Meynecke, J.-O., Dittmann, S., Ellison, A.M., Anger, K., Berger, U., Cannicci, S., Diele, K., Ewel, K.C., Field, C.D., 2007. A world without mangroves? Science 317, 41–42.

Fan, H., Liang, S., 1995. Status quo of mangrove conservation and management in China. In: He, Haiming, Fan, Hangqing (Eds.), Mangrove Research and Management in China. Science Press, Beijing, pp. 173–202.

Friess, D.A., Rogers, K., Lovelock, C.E., Krauss, K.W., Hamilton, S.E., Lee, S.Y., Lucas, R., Primavera, J., Rajkaran, A., Shi, S., 2019. The state of the world's mangrove forests: past, present, and future. Annu. Rev. Environ. Resour. 44, 89–115.

Fu, Z., Li, D., Hararuk, O., Schwalm, C., Luo, Y., Yan, L., Niu, S., 2017. Recovery time and state change of terrestrial carbon cycle after disturbance. Environ. Res. Lett. 12. https://doi.org/10.1088/1748-9326/aa8a5c.

Gallo, N.D., Victor, D.G., Levin, L.A., 2017. Ocean commitments under the Paris agreement. Nat. Clim. Chang. 7. https://doi.org/10.1038/nclimate3422.

Gao, Y., Markkanen, T., Backman, L., Henttonen, H.M., Pietikäinen, J.-P., Mäkelä, H.M., Laaksonen, A., 2014. Biogeophysical impacts of peatland forestation on regional climate changes in Finland. Biogeosciences 11, 7251–7267. https://doi.org/10.5194/bg-11-7251-2014.

Ghosh, U., Bose, S., Bramhachari, R., 2018. Living on the Edge: Climate Change and Uncertainty in the Indian Sundarbans. STEPS Working Paper 101, Brighton: STEPS Centre.

Goulden, M.L., Mcmillan, A.M.S., Winston, G.C., Rocha, A.V., Manies, K.L., Harden, J.W., Bond-Lamberty, B.P., 2011. Patterns of NPP, GPP, respiration, and NEP during boreal forest succession. Glob. Chang. Biol. 17. https://doi.org/10.1111/j.1365-2486.2010.02274.x.

Hamilton, S.E., Friess, D.A., 2018. Global carbon stocks and potential emissions due to mangrove deforestation from 2000 to 2012. Nat. Clim. Chang. 8, 240–244.

He, Y., Guan, W., Xue, D., Liu, L., Peng, C., Liao, B., Hu, J., Zhu, Q., Yang, Y., Wang, X., Zhou, G., Wu, Z., Chen, H., 2019. Comparison of methane emissions among invasive and native mangrove species in Dongzhaigang, Hainan Island. Sci. Total Environ. 697. https://doi.org/10.1016/j.scitotenv.2019.133945.

Hochard, J.P., Hamilton, S., Barbier, E.B., 2019. Mangroves shelter coastal economic activity from cyclones. Proc. Natl. Acad. Sci. U. S. A. 116. https://doi.org/10.1073/pnas.1820067116.

Holgerson, M.A., Raymond, P.A., 2016. Large contribution to inland water CO2 and CH4 emissions from very small ponds. Nat. Geosci. 9, 222–226. https://doi.org/10.1038/ngeo2654.

Holm, G.O., Perez, B.C., McWhorter, D.E., Krauss, K.W., Johnson, D.J., Raynie, R.C., Killebrew, C.J., 2016. Ecosystem level methane fluxes from tidal freshwater and brackish marshes of the Mississippi River Delta: implications for coastal wetland carbon projects. Wetlands 36. https://doi.org/10.1007/s13157-016-0746-7.

IPCC, 2014. In: Edenhofer, O., Pichs-Madruga, R. (Eds.), Climate Change 2014: Mitigation of Climate Change. Contribution of Working Group III to the Fifth Assessment Report of the Intergovernmental Panel on Climate Change. Cambridge University Press, Cambridge.

Jennerjahn, T.C., Gilman, E., Krauss, K.W., Lacerda, L.D., Nordhaus, I., Wolanski, E., 2017. Mangrove ecosystems under climate change. Mangrove Ecosystems: A Global Biogeographic Perspective. Springer, pp. 211–244.

Jia, M., Wang, Z., Zhang, Y., Mao, D., Wang, C., 2018. Monitoring loss and recovery of mangrove forests during 42 years: the achievements of mangrove conservation in China. Int. J. Appl. Earth Obs. Geoinf. 73, 535–545.

Kandel, T.P., Lærke, P.E., Hoffmann, C.C., Elsgaard, L., 2019. Complete annual CO2, CH4, and N2O balance of a temperate riparian wetland 12 years after rewetting. Ecol. Eng. 127, 527–535. https://doi.org/10.1016/j.ecoleng.2017.12.019.

Kang, W., Zhao, Z., Tian, D., He, J., Deng, X., 2008. CO2 exchanges between mangrove and shoal wetland ecosystems and atmosphere in Guangzhou. Chin. J. Appl. Ecol. 19, 2605–2610.

Kljun, N., Calanca, P., Rotach, M.W., Schmid, H.P., 2015. A simple two-dimensional parameterisation for flux footprint prediction (FFP). Geosci. Model Dev. 8. https://doi.org/10.5194/gmd-8-3695-2015.

Knox, S.H., Jackson, R.B., Poulter, B., McNicol, G., Fluet-Chouinard, E., Zhang, Z., Hugelius, G., Bousquet, P., Canadell, J.G., Saunois, M., Papale, D., Chu, H., Keenan, T.F.,

Baldocchi, D., Torn, M.S., Mammarella, I., Trotta, C., Aurela, M., Bohrer, G., Campbell, D.I., Cescatti, A., Chamberlain, S., Chen, J., Chen, W., Dengel, S., Desai, A.R., Euskirchen, E., Friborg, T., Gasbarra, D., Goded, I., Goeckede, M., Heimann, M., Helbig, M., Hirano, T., Hollinger, D.Y., Iwata, H., Kang, M., Klatt, J., Krauss, K.W., Kutzbach, L., Lohila, A., Mitra, B., Morin, T.H., Nilsson, M.B., Niu, S., Noormets, A., Oechel, W.C., Peichl, M., Peltola, O., Reba, M.L., Richardson, A.D., Runkle, B.R.K., Ryu, Y., Sachs, T., Schäfer, K.V.R., Schmid, H.P., Shurpali, N., Sonnentag, O., Tang, A.C.I., Ueyama, M., Vargas, R., Vesala, T., Ward, E.J., Windham-Myers, L., Wohlfahrt, G., Zona, D., 2019. FLUXNET-CH4 synthesis activity objectives, observations, and future directions. Bull. Am. Meteorol. Soc. 100, 2607–2632. https://doi.org/10.1175/BAMS-D-18-0268.1.

Krauss, K.W., Holm, G.O., Perez, B.C., McWhorter, D.E., Cormier, N., Moss, R.F., Johnson, D.J., Neubauer, S.C., Raynie, R.C., 2016. Component greenhouse gas fluxes and radiative balance from two deltaic marshes in Louisiana: pairing chamber techniques and eddy covariance. J. Geophys. Res. Biogeosci. 121. https://doi.org/10.1002/2015JG003224.

Leopold, A., Marchand, C., Renchon, A., Deborde, J., Quiniou, T., Allenbach, M., 2016. Agricultural and Forest meteorology net ecosystem CO2 exchange in the "coeur de voh" mangrove, New Caledonia : effects of water stress on mangrove productivity in a semi-arid climate. Agric. For. Meteorol. 223, 217–232. https://doi.org/10.1016/j.agrformet.2016.04.006.

Li, Q., Lu, W., Chen, H., Luo, Y., Lin, G., 2014. Differential responses of net ecosystem exchange of carbon dioxide to light and temperature between spring and neap tides in subtropical mangrove forests. Sci. World J. 2014, 943697. https://doi.org/10.1155/2014/943697.

Li, T., Huang, Y., Zhang, W., Song, C., 2010. CH4MODwetland: a biogeophysical model for simulating methane emissions from natural wetlands. Ecol. Model. 221. https://doi.org/10.1016/j.ecolmodel.2009.05.017.

Li, T., Xie, B., Wang, G., Zhang, W., Zhang, Q., Vesala, T., Raivonen, M., 2016. Field-scale simulation of methane emissions from coastal wetlands in China using an improved version of CH4MODwetland. Sci. Total Environ. 559, 256–267. https://doi.org/10.1016/j.scitotenv.2016.03.186.

Liu, J., Lai, D.Y.F., 2019. Subtropical mangrove wetland is a stronger carbon dioxide sink in the dry than wet seasons. Agric. For. Meteorol. 278. https://doi.org/10.1016/j.agrformet.2019.107644.

Liu, J., Zhou, Y., Valach, A., Shortt, R., Kasak, K., Rey-Sanchez, C., Hemes, K.S., Baldocchi, D., Lai, D.Y.F., 2020. Methane emissions reduce the radiative cooling effect of a subtropical estuarine mangrove wetland by half. Glob. Chang. Biol. 26, 4998–5016. https://doi.org/10.1111/gcb.15247.

Lovelock, C.E., Duarte, C.M., 2019. Dimensions of blue carbon and emerging perspectives. Biol. Lett. https://doi.org/10.1098/rsbl.2018.0781.

Macreadie, P.I., Nielsen, D.A., Kelleway, J.J., Atwood, T.B., Seymour, J.R., Petrou, K., Connolly, R.M., Thomson, A.C.G., Trevathan-Tackett, S.M., Ralph, P.J., 2017. Can we manage coastal ecosystems to sequester more blue carbon? Front. Ecol. Environ. 15, 206–213. https://doi.org/10.1002/fee.1484.

Massman, W.J., 2000. A simple method for estimating frequency response corrections for eddy covariance systems. Agric. For. Meteorol. https://doi.org/10.1016/S0168-1923(00)00164-7.

Moncrieff, J., Clement, R., Finnigan, J., Meyers, T., 2004. Averaging, detrending, and filtering of eddy covariance time series. In: LEE, X., Massman, W., Law, B (Eds.), Handbook of Micrometeorology: A Guide for Surface Flux Measurement and Analysis. Kluwer Academic Publisher, Dordrecht.

Nakai, T., Shimoyama, K., 2012. Ultrasonic anemometer angle of attack errors under turbulent conditions. Agric. For. Meteorol. 162–163. https://doi.org/10.1016/j.agrformet.2012.04.004.

Nellemann, C., Corcoran, E., Duarte, C., Valdés, L., De Young, C., Fonseca, L., Grimsditch, G., 2009. Blue Carbon: The Role of Healthy Oceans in Binding Carbon: A Rapid Response Assessment. United Nations Environment Programme, Arendal, Norway.

Ngoc, V., Sigit, N., Daniel, D.S., Purbopuspito, J., Mackenzie, R.A., 2016. Carbon stocks in artificially and naturally regenerated mangrove ecosystems in the Mekong Delta. Wetl. Ecol. Manag. 24, 231–244. https://doi.org/10.1007/s11273-015-9479-2.

Phan, S.M., Nguyen, H.T.T., Nguyen, T.K., Lovelock, C., 2019. Modelling above ground biomass accumulation of mangrove plantations in Vietnam. For. Ecol. Manag. 432. https://doi.org/10.1016/j.foreco.2018.09.028.

Poffenbarger, H.J., Needelman, B.A., Megonigal, J.P., 2011. Salinity influence on methane emissions from tidal marshes. Wetlands 31. https://doi.org/10.1007/s13157-011-0197-0.

Qiu, P., Xu, S., Fu, Y., Xie, G., 2011. A primary study on plant community of Wanqingsha Semi-constructed wetland in Nansha District of Guangzhou City. Ecol. Sci. 30, 43–50.

Reichstein, M., Kätterer, T., Andrén, O., Ciais, P., Schulze, E.D., Cramer, W., Papale, D., Valentini, R., 2005. Temperature sensitivity of decomposition in relation to soil organic matter pools: critique and outlook. Biogeosciences 2. https://doi.org/10.5194/bg-2-317-2005.

Rodda, S.R., Thumaty, K.C., Jha, C.S., Dadhwal, V.K., 2016. Seasonal variations of carbon dioxide, water vapor and energy fluxes in tropical indian mangroves. Forest 7, 1–18. https://doi.org/10.3390/f7020035.

Roehm, C.L., 2005. Respiration in wetland ecosystems. In: del Giorgio, P.A., Williams, P.J. (Eds.), Respiration in Aquatic Ecosystems. Oxford University Press, Oxford.

Rosentreter, J.A., Maher, D.T., Erler, D.V., Murray, R., Eyre, B.D., 2018a. Factors controlling seasonal CO2 and CH4 emissions in three tropical mangrove-dominated estuaries in Australia. Estuar. Coast. Shelf Sci. 215, 69–82.

Rosentreter, J.A., Maher, D.T., Erler, D.V., Murray, R.H., Eyre, B.D., 2018b. Methane emissions partially offset "blue carbon" burial in mangroves. Sci. Adv. 4, eaao4985.

Sasmito, S.D., Taillardat, P., Clendenning, J.N., Cameron, C., Friess, D.A., Murdiyarso, D., Hutley, L.B., 2019. Effect of land-use and land-cover change on mangrove blue carbon: a systematic review. Glob. Chang. Biol. 25, 4291–4302. https://doi.org/10.1111/gcb.14774.

Schile, L.M., Kauffman, J.B., Crooks, S., Fourqurean, J.W., Glavan, J., Megonigal, J.P., 2017. Limits on carbon sequestration in arid blue carbon ecosystems. Ecol. Appl. 27. https://doi.org/10.1002/eap.1489.

Shen, X., Liu, B., Jiang, M., Lu, X., 2020. Marshland loss warms local land surface temperature in China. Geophys. Res. Lett. 47, e2020GL087648. https://doi.org/10.1029/2020GL087648.

Sievers, M., Brown, C.J., Tulloch, V.J.D., Pearson, R.M., Haig, J.A., Turschwell, M.P., Connolly, R.M., 2019. The role of vegetated coastal wetlands for marine megafauna conservation. Trends Ecol. Evol. https://doi.org/10.1016/j.tree.2019.04.004.

Singh, S.N., Kulshreshtha, K., Agnihotri, S., 2000. Seasonal dynamics of methane emission from wetlands. Chemosphere Global Change Sci. 2. https://doi.org/10.1016/S1465-9972(99)00046-X.

Fan, Song-Miao, Wofsy, S.C., Bakwin, P.S., Jacob, D.J., Fitzjarrald, D.R., 1990. Atmosphere-biosphere exchange of CO2 and O3 in the Central Amazon forest. J. Geophys. Res. 95. https://doi.org/10.1029/jd095id10p16851.

Song, Y., Xu, S., Liu, X., Al, E., 2016. Time and space differences of water environmental quality of the mangrove Wetland Park in Nansha: based on the improved twice-slope clustering method. Sci. Geogr. Sin. 36, 303–311.

Taillardat, P., Friess, D.A., Lupascu, M., 2018. Mangrove blue carbon strategies for climate change mitigation are most effective at the national scale. Biol. Lett. 14, 20180251.

Temmerman, S., Meire, P., Bouma, T.J., Herman, P.M.J., Ysebaert, T., De Vriend, H.J., 2013. Ecosystem-based coastal defence in the face of global change. Nature https://doi.org/10.1038/nature12859.

Vickers, D., Mahrt, L., 1997. Quality control and flux sampling problems for tower and aircraft data. J. Atmos. Ocean. Technol. 14. https://doi.org/10.1175/1520-0426(1997)014<0512:QCAFSP>2.0.CO;2.

Wang, W., Liu, H., Li, Y., Su, J., 2014. Development and management of land reclamation in China. Ocean Coast. Manag. 102. https://doi.org/10.1016/j.ocecoaman.2014.03.009.

Webb, E.K., Pearman, G.I., Leuning, R., 1980. Correction of flux measurements for density effects due to heat and water vapour transfer. Q. J. R. Meteorol. Soc. https://doi.org/10.1002/qj.49710644707.

Wilczak, J.M., Oncley, S.P., Stage, S.A., 2001. Sonic anemometer tilt correction algorithms. Bound.-Layer Meteorol. https://doi.org/10.1023/A:1018966204465.

Wutzler, T., Lucas-Moffat, A., Migliavacca, M., Knauer, J., Sickel, K., Šigut, L., Menzer, O., Reichsteinet, M., 2018. Basic and extensible post-processing of eddy covariance flux data with REddyProc. Biogeosciences 15, 5015–5030. https://doi.org/10.5194/bg-15-5015-2018.

Xu, Y., Liao, B., Jiang, Z., Xin, K., Xiong, Y., Guan, W., 2020. Emission of greenhouse gases (CH4 and CO2) into the atmosphere from restored mangrove soil in South China. J. Coast. Res. 37, 52–58. https://doi.org/10.2112/jcoastres-d-20-00054.1.

Ye, Y., Lv, C., Lin, P., 2000. Seasonal and spatial changes of methane emissions from mangrove wetlands in Hainan Island and Xiamen. Chin. J. Atmos. Sci. 24, 152–156.

Zhu, X., Qin, Z., Song, L., 2021. How land-sea interaction of tidal and sea breeze activity affect mangrove net ecosystem exchange ? J. Geophys. Res. Atmos. 126. https://doi.org/10.1029/2020JD034047.

Zhu, X., Sun, C., Qin, Z., 2021. Drought-induced salinity enhancement weakens mangrove greenhouse gas cycling. J. Geophys. Res. Biogeosci. 126. https://doi.org/10.1029/2021jg006416.